Effects of Pro → Peptoid Residue Substitution on Cell Selectivity and Mechanism of Antibacterial Action of Tritrpticin-Amide Antimicrobial Peptide†

Wan Long Zhu,‡ Hongliang Lan,‡ Yoonkyung Park,‡ Sung-Tae Yang,§ Jae Il Kim,§ Il-Seon Park,‡,|| Ho Jin You,‡ Jung Sup Lee,‡ Yong Sun Park,⊥ Yangmee Kim,@ Kyung-Soo Hahm,‡,|| and Song Yub Shin*,‡,||

Department of Bio-Materials, Graduate School and Research Center for Proteineous Materials, Chosun University, Gwangju 501-759, Korea, Department of Life Science, Gwangju Institute of Science and Technology, Gwangju 500-712, Korea, Department of Cellular and Molecular Medicine, School of Medicine, Chosun University, Gwangju 501-759, Korea, Department of Chemistry, Konkuk University, Seoul 143-701, Korea, and Department of Bioscience and Biotechnology, Bio/Molecular Informatics Center, IBST, Konkuk University, Seoul 143-701, Korea

Received March 11, 2006; Revised Manuscript Received August 24, 2006

ABSTRACT: To investigate the effect of Pro → peptoid residue substitution on cell selectivity and the mechanism of antibacterial action of Pro-containing β-turn antimicrobial peptides, we synthesized tritrpticin-amide (TP, VRRFPWWWPFLRR-NH_2) and its peptoid residue-substituted peptides in which two Pro residues at positions 5 and 9 are replaced with Nleu (Leu peptoid residue), Nphe (Phe peptoid residue), or Nlys (Lys peptoid residue). Peptides with Pro → Nphe (TPf) or Pro → Nleu substitution (TPl) retained antibacterial activity but had significantly higher toxicity to mammalian cells. In contrast, Pro → Nlys substitution (TPk) increased the antibacterial activity but decreased the toxicity to mammalian cells. Tryptophan fluorescence studies indicated that the bacterial cell selectivity of TPk is closely correlated with a preferential interaction with negatively charged phospholipids. Interestingly, TPk was much less effective at depolarizing of the membrane potential of *Staphylococus aureus* and *Escherichia coli* spheroplasts and causing the leakage of a fluorescent dye entrapped within negatively charged vesicles. Furthermore, confocal laser-scanning microscopy showed that TPk effectively penetrated the membrane of both *E. coli* and *S. aureus* and accumulated in the cytoplasm, whereas TP and TPf did not penetrate the cell membrane but remained outside or on the cell membrane. These results suggest that the bactericidal action of TPk is due to inhibition of the intracellular components after penetration of the bacterial cell membrane. In addition, TPK with Lys substitution effectively depolarized the membrane potential of *S. aureus* and *E. coli* spheroplasts. TPK induced rapid and effective dye leakage from bacterial membrane-mimicking liposomes and did not penetrate the bacterial cell membranes. These results suggested that the ability of TPk to penetrate the bacterial cell membranes appears to involve the dual effects that are related to the increase in the positive charge and the peptide's backbone change by peptoid residue substitution. Collectively, our results showed that Pro → Nlys substitution in Pro-containing β-turn antimicrobial peptides is a promising strategy for the design of new short bacterial cell-selective antimicrobial peptides with intracellular mechanisms of action.

Antimicrobial peptides play an important role in the innate immunity system of many higher organisms such as plants, insects, amphibians, and mammals (*1*−*5*). Due to the alarming emergence of pathogenic organisms resistant to conventional antibiotics, antimicrobial peptides are being intensively studied with the objective of developing a new class of antimicrobial drug. The 13-residue cationic tritrpticin (VRRFPWWWPFLRR) is a member of the cathelicidin family, a group of diverse antimicrobial peptides found in neutrophil granules (*6*). Tritrpticin has a unique composition, consisting of 30% arginine, 23% tryptophan, and 15% proline. Tritrpticin may be a candidate for drug development because it has a broad spectrum of antimicrobial activity against Gram-positive and Gram-negative bacteria and some fungi. Its therapeutic potential, however, is limited by its relatively strong hemolytic activity against human erythrocytes (*6*−*8*).

Tritrpticin contains two Pro residues at positions 5 and 9. Nuclear magnetic resonance (NMR) study has shown that, in membrane-mimicking sodium dodecyl sulfate (SDS)[1] micelles, tritrpticin adopts a unique structure with two adjacent β-turns around Pro^5 and Pro^9. The hydrophobic residues are clustered together and are clearly separated from the basic Arg residues, resulting in an amphipathic β-turn

† This study was supported by an ERC grant of the Ministry of Science and Technology, Korea, and the Korea Science and Engineering Foundation through the Research Center for Proteineous Materials (R11-2000-083-00000-0) and by a Next Generation New Technology Development Program Grant (10027891) of the Ministry of Commerce, Industry and Energy (MOCIE) of South Korea.

* To whom correspondence should be addressed. Telephone: 82-62-230-6769. Fax: 82-62-227-8345. E-mail: syshin@chosun.ac.kr.

‡ Graduate School and Research Center for Proteineous Materials, Chosun University.

§ Gwangju Institute of Science and Technology.

|| School of Medicine, Chosun University.

⊥ Department of Chemistry, Konkuk University.

@ Department of Bioscience and Biotechnology, Bio/Molecular Informatics Center, IBST, Konkuk University.

10.1021/bi060487+ CCC: $33.50
Published on Web 10/10/2006

Table 1: Amino Acid Sequences of Tritrpticin-Amide and Its Peptoid Residue-Substituted Peptides[a]

Peptide	Sequence	Molecular mass (Da)		Retention Time (min)[c]
		Calculated	Observed[b]	
Tritrpticin	VRRFPWWWPFLRR	1902.2	1903.3	31.92
TP	VRRFPWWWPFLRR-NH_2	1901.2	1903.2	32.57
TPl	VRRF**l**WWW**l**FLRR-NH_2	1933.3	1935.3	35.31
TPf	VRRF**f**WWW**f**FLRR-NH_2	2001.4	2002.0	36.05
TPk	VRRF**k**WWW**k**FLRR-NH_2	1963.3	1965.2	27.47
TPK	VRRFKWWWKFLRR-NH_2	1963.3	1963.4	28.75

[a] **l** is Nleu [$(CH_3)_2$-CH-NH-CH_2-COOH], **f** Nphe (H_5C_6-CH_2-NH-CH_2-COOH), and **k** Nlys [NH_2-$(CH_2)_4$-NH-CH_2-COOH]. [b] Molecular masses of the peptides from MALDI-TOF MS. [c] This was obtained using C_{18} RP-HPLC with a linear gradient from 5 to 60% acetonitrile in water, both containing 0.05% TFA (v/v).

structure (*9*). The Pro residue plays a critical role in determining the secondary structure of the peptides because it induces a reversal in backbone conformation, resulting in the breaking of helices as well as in the formation of β-turns. Like Pro, peptoid (*N*-alkylglycyl) residues are imino acids because their side chains are shifted from the α-carbon position to the N-position. Peptoid residue-containing peptides generally exhibit greater proteolytic stability and bioavailability than their respective peptide analogues (*10*). They have been found to be potential drugs as discovered from peptidomimetic libraries (*11*) and determined to be effective molecular transporters via their enhancement of the cellular uptake of agents (*12*). In another interesting application, the Leu peptoid residue (Nleu) has been introduced as a substituted proline into synthetic collagen-like structures (*13*).

Like proline, peptoid residues have β-turn-forming potential as well as an ability to break α-helices because of they lack an amide proton for forming intramolecular hydrogen bonds (*14*, *15*). To our knowledge, previous studies have not addressed the effect of Pro → peptoid residue substitution on cell selectivity and the mechanism of antibacterial action of amphipathic β-turn antimicrobial peptides containing Pro residues such as tritrpticin. To address these issues, we synthesized tritrpticin-amide (TP, VRRFPWWWPFLRR-NH_2) and its peptoid residue-substituted peptides, which have the sequence VRRFXWWWX-FLRR-NH_2, wherein X represents substitutions of Pro with Nleu (Leu peptoid residue), Nphe (Phe peptoid residue), or Nlys (Lys peptoid residue).

We assessed the cell selectivity of the peptides by measuring the bactericidal activity against six bacterial strains, the hemolytic activity against human red blood cells, and the cytotoxicity against human cervical carcinoma HeLa and mouse fibroblastic NIH-3T3 cells. We also used tryptophan fluorescence spectroscopy and model membrane systems mimicking the bacterial and mammalian cytoplasmic membranes to investigate the molecular basis for the selectivity of the peptides. We further examined the secondary structures of the peptides in the SDS micelles and bacterial membrane-mimicking liposomes using circular dichroism (CD) spectroscopy, and we investigated the mechanism of the peptides' antibacterial action by fluorescent dye leakage, membrane potential depolarization, confocal laser-scanning microscopy, and gel retardation. These peptoid residue-containing antimicrobial peptides offer unique insight into how peptides interact with model membranes or intact bacterial or mammalian cell membranes, and the results provide important information about the design of possible bacterial cell-selective antimicrobial peptides for therapeutic applications.

MATERIALS AND METHODS

Materials. Rink amide 4-methylbenzhydrylamine resin, fluoren-9-ylmethoxycarbonyl (Fmoc) amino acids, Fmoc-ϵ-Ahx-OH, and other reagents for the peptide synthesis were purchased from Calibochem-Novabiochem (La Jolla, CA). Egg yolk L-α-phosphatidylcholine (EYPC), egg yolk L-α-phosphatidyl-DL-glycerol (EYPG), acrylamide, calcein, 3-(4,5-dimethylthiazol-2-yl)-2,5-diphenyl-2*H*-tetrazolium bromide (MTT), cholesterol, and gramicidin D were supplied by Sigma Chemical Co. (St. Louis, MO). 3,3′-Dipropylthiadicarbocyanine iodide ($diSC_3$-5) was obtained from Molecular Probes (Eugene, OR). DMEM and fetal bovine serum (FBS) were supplied from HyClone (SeouLin Bioscience). Human cervical carcinoma HeLa and mouse fibroblastic NIH-3T3 cells were purchased from the American Type Culture Collection (Manassas, VA). All other reagents were analytical grade. The buffers were prepared in double glass-distilled water.

Peptide Synthesis and Purification. Tritrpticin-amide and its peptoid-containing peptides and FITC-labeled peptides (FITC-labeled aminocaproic acid peptides) were prepared by the standard Fmoc-based solid-phase method on rink amide 4-methylbenzhydrylamine resin (0.54 mmol/g). Fmoc-Nleu-OH, Fmoc-Nphe-OH, and Fmoc-Nlys-OH were synthesized using the previous methods (*14*, *15*). The crude peptides were purified by RP-HPLC using a Shim-pack C_{18} column (15 μm, 20 mm × 250 mm; Shimadzu). The purified peptides were shown to be homogeneous (>98%) by analytical RP-HPLC on a Shim-pack C_{18} column (5 μm, 4.6 mm × 250 mm). Matrix-assisted laser desorption ionization time-of-flight mass spectrometry (MALDI-TOF MS) (Shimadzu) was used to confirm their molecular weight (Table 1).

Antimicrobial Activity. The antimicrobial activities of the peptides were examined in sterile 96-well plates in a final

[1] Abbreviations: CD, circular dichroism; CFU, colony-forming units; $diSC_3$-5, 3,3′-dipropylthiadicarbocyanine iodide; DMEM, Dulbecco's modified Eagle's medium; EYPC, egg yolk L-α-phosphatidylcholine; EYPG, egg yolk L-α-phosphatidyl-DL-glycerol; FBS, fetal bovine serum; FITC, fluorescein isothiocyanate; Fmoc, fluoren-9-ylmethoxycarbonyl; h-RBC, human red blood cells; LUVs, large unilamellar vesicles; MALDI-TOF MS, matrix-assisted laser desorption ionization time-of-flight mass spectrometry; MIC, minimal inhibitory concentration; MTT, 3-(4,5-dimethylthiazol-2-yl)-2,5-diphenyl-2*H*-tetrazolium bromide; RP-HPLC, reverse-phase high-performance liquid chromatography; PBS, phosphate-buffered saline; SDS, sodium dodecyl sulfate; SUVs, small unilamellar vesicles.

volume of 200 μL as follows. Aliquots (100 μL) of a bacterial suspension at 2×10^6 colony-forming units (CFU)/mL in 1% peptone were added to 100 μL of a peptide solution (serial 2-fold dilutions in 1% peptone). After incubation for 18−20 h at 37 °C, the inhibition of bacterial growth was assessed by measuring the absorbance at 620 nm with a Microplate autoreader EL 800 (Bio-Tek Instruments). The minimal inhibitory concentration (MIC) was defined as the lowest concentration of peptide that inhibited growth. Bacterial strains were purchased from the Korean Collection for Type Cultures (KCTC) at the Korea Research Institute of Bioscience and Biotechnology and included three types of Gram-positive bacteria [*Bacillus subtilis* (KCTC 3068), *Staphylococcus epidermidis* (KCTC 1917), and *Staphylococcus aureus* (KCTC 1621)] and three types of Gram-negative bacteria [*Escherichia coli* (KCTC 1682), *Pseudomonas aeruginosa* (KCTC 1637), and *Salmonella typhimurium* (KCTC 1926)].

Hemolytic Activity. Hemolytic activity of the peptides was tested against human red blood cells (h-RBC). Fresh h-RBC were washed three times with phosphate-buffered saline (PBS) [35 mM phosphate buffer containing 150 mM NaCl (pH 7.4)] by centrifugation for 10 min at 1000*g* and resuspended in PBS. The peptide solutions were then added to 50 μL of h-RBC in PBS to give a final volume of 100 μL and a final erythrocyte concentration of 4% (v/v). The resulting suspension was incubated with agitation for 1 h at 37 °C. The samples were centrifuged at 1000*g* for 5 min. Release of hemoglobin was monitored by measuring the absorbance of the supernatant at 405 nm. Controls for no hemolysis (blank) and 100% hemolysis consisted of human red blood cells suspended in PBS and 0.1% Triton X-100, respectively.

Cytotoxicity against Mammalian Cells. Human cervical carcinoma HeLa and mouse fibroblastic NIH-3T3 cells were cultured in DMEM with 10% FBS. The cells were maintained under 5% CO_2 at 37 °C. Cytotoxicity against mammalian cells of the peptides was determined by the MTT assay as previously reported (*16*) with minor modifications. The cells were seeded on 96-well microplates at a density of 2×10^4 cells/well in 150 μL of DMEM containing 10% FBS. The plates were then incubated for 24 h at 37 °C in a 5% CO_2 atmosphere. Twenty microlilters of peptide solution (serial 2-fold dilutions in DMEM) was added, and the plates were incubated for a further 2 days. Wells containing cells without peptides served as controls. Subsequently, 20 μL of an MTT solution (5 mg/mL) was added to each well, and the plates were incubated for a further 4 h at 37 °C. The precipitated MTT formazan was dissolved in 40 μL of 20% (w/v) SDS containing 0.01 M HCl overnight. The absorbance at 570 nm was measured using a microplate ELISA reader (Molecular Devices, Sunnyvale, CA). Percent cell survival was expressed as a percent ratio of A_{570} of cells treated with peptide over cells only.

CD Spectra. The CD spectra of peptides were recorded in 10 mM sodium phosphate buffer (pH 7.2) with and without 30 mM SDS or 1 mM EYPC/EYPG (7:3, w/w) SUVs by utilizing a Jasco (Tokyo, Japan) J-715 CD spectrophotometer calibrated routinely with 10-camphorsulfonic acid. The samples were scanned at room temperature in a capped quartz cuvette of 1 mm path length cells in the wavelength range of 250−190 nm.

Preparation of Small Unilamellar Vesicles (SUVs). Small unilamellar vesicles were prepared by a standard procedure with required amounts of either EYPC/EYPG (7:3, w/w) or EYPC/cholesterol (10:1, w/w) for tryptophan fluorescence. Dry lipids were dissolved in chloroform in a small glass vessel. Solvents were removed by rotary evaporation to form a thin film on the wall of a glass vessel. The dried thin film was resuspended in Tris-HCl buffer by vortex mixing. The lipid dispersions were then sonicated in an ice/water mixture for 10−20 min with a titanium-tip ultrasonicator until the solution became transparent.

Dye Leakage Assay. Calcein-entrapped LUVs composed of EYPC/EYPG (7:3, w/w) were prepared by vortexing the dried lipid in dye buffer solution [70 mM calcein, 10 mM Tris, 150 mM NaCl, and 0.1 mM EDTA (pH 7.4)]. The suspension was frozen and thawed in liquid nitrogen for ten cycles and extruded through polycarbonate filters (two stacked 100 nm pore size filters) with a LiposoFast extruder (Avestin, Inc.). Untrapped calcein was removed by gel filtration on a Sephadex G-50 column. Usually lipid vesicles are diluted to approximately 10-fold after passing through a Sephadex G-50 column. The eluted calcein-entrapped vesicles were diluted further to the desired final lipid concentration for the experiment. The leakage of calcein from the LUVs was monitored by measuring the fluorescence intensity at an excitation wavelength of 490 nm and an emission wavelength of 520 nm on a model RF-5301PC spectrophotometer (Shimadzu). For determination of 100% dye release, 10% Triton X-100 in Tris buffer (20 μL) was added to dissolve the vesicles. The percentage of dye leakage caused by the peptides was calculated as follows:

$$\text{dye leakage (\%)} = 100[(F - F_0)/(F_t - F_0)]$$

where F is the fluorescence intensity achieved by the peptides and F_0 and F_t are fluorescence intensities without the peptides and with Triton X-100, respectively.

Tryptophan Fluorescence Blue Shift. In the tryptophan fluorescence blue shift and quenching experiments, small unilamellar vesicles (SUVs) were used to minimize differential light scattering effects (*17*, *18*). Each peptide (final concentration of 3 μM) was added to 3 mL of 10 mM Tris buffer [0.1 mM EDTA and 150 mM NaCl (pH 7.4)] containing 0.6 mM liposomes, and the peptide/liposome mixture was allowed to interact at 20 °C for 10 min. The fluorescence was excited at 280 nm, and the emission was scanned from 300 to 400 nm.

Quenching of Trp Emission by Acrylamide. For fluorescence quenching experiments, acrylamide was used as the quencher. To reduce absorbance by acrylamide, excitation of Trp at 295 nm instead of 280 nm was used (*19*, *20*). Aliquots of the 4.0 M solution of this water-soluble quencher were added to the peptide in the absence or presence of liposomes at a peptide:lipid molar ratio of 1:200. The acrylamide concentration in the cuvette was from 0.04 to 0.21 M. The effect of acrylamide on the fluorescence of each peptide was analyzed with a Stern−Volmer equation:

$$F_0/F = 1 + K_{sv}[Q]$$

where F_0 and F represent the fluorescence intensities in the absence and the presence of acrylamide, respectively, K_{sv} is

Table 2: Minimal Inhibitory Concentrations of the Peptides[a]

peptide	minimal inhibitory concentration (μM)					
	E. coli (KCTC1682)	*S. typhimurium* (KCTC1926)	*P. aeruginosa* (KCTC1637)	*B. subtilis* (KCTC3068)	*S. aureus* (KCTC1261)	*S. epiderrmidis* (KCTC1917)
tritrpticin	8	16	16	4	4	4
TP	8	8	8	1	2	1
TPl	8	16	16	1	2	1
TPf	8	8	8	1	2	1
TPk	2	4	4	1	1	1
TPK	2	2	4	0.5	1	0.5

[a] Each MIC was determined in three independent experiments performed in triplicate with a standard deviation of 9.8%.

the Stern−Volmer quenching constant, and [Q] is the concentration of acrylamide.

Membrane Depolarization Assay with Bacteria. The membrane depolarization activity of the peptides was determined with Gram-positive bacteria and Gram-negative bacterial spheroplasts using the experimental conditions described previously (*21*, *22*). Gram-positive bacteria, *S. aureus*, was grown at 37 °C with agitation to mid-log phase ($OD_{600} = 0.4$). The cells were centrifuged, washed twice with buffer [20 mM glucose and 5 mM HEPES (pH 7.4)], and resuspended to an OD_{600} of 0.05 in a similar buffer containing 0.1 M KCl. Spheroplasts of Gram-negative *E. coli* bacteria (lipopolysaccharide- and peptidoglycan-free bacteria) were prepared by the osmotic shock procedure as follows. Cells from cultures grown to an OD_{600} of 0.8 were harvested by centrifugation and washed twice with 10 mM Tris-H_2SO_4 and 25% sucrose (pH 7.5). The cells were washed and resuspended in the washing buffer containing 1 mM EDTA. After a 10 min incubation at 20 °C with rotary mixing, the cells were collected by centrifugation and resuspended immediately in cold (4 °C) water. After a 10 min incubation at 4 °C with rotary mixing, the spheroplasts were then collected by centrifugation. The spheroplasts were then resuspended to an OD_{600} of 0.1 in a buffer containing 20 mM glucose, 5 mM HEPES, and 0.1 M KCl (pH 7.4). The prepared cells of *S. aureus* or *E. coli* spheroplasts were incubated with 20 nM $diSC_3$-5 until a stable reduction of fluorescence was achieved (around 60 min), indicating the incorporation of the dye into the bacterial membrane. The peptides were then added from the stock solution (1 mg/mL) and dissolved in the buffer to achieve the desired concentration. Membrane depolarization was monitored by the change in the intensity of fluorescence emission of the membrane potential-sensitive dye $diSC_3$-5 (excitation wavelength $\lambda_{ex} = 622$ nm; emission wavelength $\lambda_{em} = 670$ nm) after different concentrations of peptides were added. Full dissipation of the membrane potential was obtained by adding gramicidin D (for *S. aureus*, the final concentration is 0.2 nM) or melittin (for *E. coli* spheroplasts, the final concentration is 0.5 μM). The membrane potential dissipating activity of the peptides is expressed as follows:

$$\% \text{ inhibition} = 100[(F_p - F_0)/(F_g - F_0)]$$

where F_0 is the stable fluorescence value after addition of the $diSC_3$-5 dye, F_p is the fluorescence value 2 min after addition of the peptides, and F_g is the fluorescence signal after the addition of gramicidin D (for *S. aureus*) or melittin (for *E. coli* spheroplasts).

Confocal Laser-Scanning Microscopy. *E. coli* and *S. aureus* cells in mid-logarithmic phase were prepared. *E. coli* and *S. aureus* cells (10^7 CFU/mL) in 10 mM sodium phosphate buffer (NAPB, pH 7.4) were incubated with FITC-labeled peptides (5 μg/mL) at 37 °C for 30 min. After being incubated, the cells were washed with 10 mM NAPB and immobilized on a glass slide. The FITC-labeled peptides were observed with an Olympus IX 70 confocal laser-scanning microscope (Japan). Fluorescent images were obtained with a 488 nm band-pass filter for excitation of FITC.

DNA Binding Assay. Gel retardation experiments were performed by mixing 100 ng of the plasmid DNA (pBluescript II SK^+) with increasing amounts of peptide in 20 μL of binding buffer [5% glycerol, 10 mM Tris-HCl (pH 8.0), 1 mM EDTA, 1 mM dithiothreitol, 20 mM KCl, and 50 μg/mL bovine serum albumin]. The reaction mixtures were incubated at room temperature for 1 h. Subsequently, 4 μL of native loading buffer was added [10% Ficoll 400, 10 mM Tris-HCl (pH 7.5), 50 mM EDTA, 0.25% bromophenol blue, and 0.25% xylene cyanol], and a 20 μL aliquot was subjected to a 1% agarose gel electrophoresis in 0.5× Tris borate-EDTA buffer [45 mM Tris-borate and 1 mM EDTA (pH 8.0)]. The plasmid DNA used in this experiment was purified by CsCl gradient ultracentrifugation to select the closed circular form of the plasmid.

RESULTS

Peptide Design. To investigate the effect of Pro → peptoid residue substitution in tritrpticin-amide on cell selectivity and the mechanism of antibacterial action, we synthesized a series of peptoid residue-substituted peptides, in which two Pro residues at positions 5 and 9 of tritrpticin-amide were replaced with Nleu (Leu peptoid residue), Nphe (Phe peptoid residue), or Nlys (Lys peptoid residue). In addition, to compare the effect of Pro → Nlys substitution and Pro → Lys substitution in tritrpticin-amide on their biological activity and mode of antibacterial action, TPK in which two Pro residues are replaced with two lysine residues was synthesized. The amino acid sequences of all peptides are summarized in Table 1.

Antibacterial and Hemolytic Activities. The antimicrobial activities of the peptides against bacterial strains, including three Gram-negative and three Gram-positive species, were investigated using the broth microdilution method (*23*−*25*). The MIC values of the peptides against these bacterial strains are summarized in Table 2. TPl and TPf exhibited antibacterial activities similar to those of TP against all of the bacterial strains that were tested. In contrast, TPk and TPK exhibited 2−4-fold higher activity than TP. The hemolytic activity of the peptides against human erythrocytes was also determined. Figure 1 shows dose−response curves for the hemolytic activities of the peptides. TPl and TPf exhibited greater

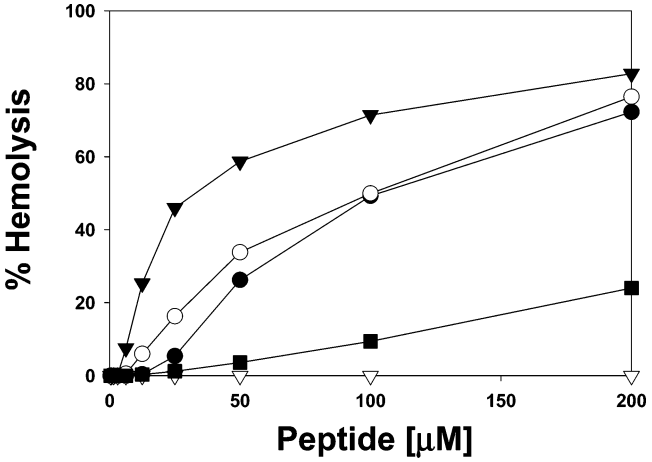

FIGURE 1: Dose−response curves of the hemolytic activity of the peptides toward human erythrocytes: TP (●), TPl (○), TPf (▼), TPk (▽), and TPK (■).

hemolytic activity than TP. In contrast, TPK and TPk exhibited decreased hemolytic activity. Interestingly, TPk did not cause any hemolysis at 200 μM, but TPK caused 20% hemolysis.

Cytotoxicity against Mammalian Cells. We examined the ability of the peptides to inhibit the growth of two mammalian cell lines (human cervical carcinoma HeLa and mouse fibroblastic NIH-3T3 cells). The growth inhibition dose−response curves for the peptides are shown in Figure 2. The IC_{50} is the peptide concentration causing 50% inhibition of cell growth compared to untreated control cells (Table 3). TPl, TPf, and TPK were much more cytotoxic than TP and TPk. In particular, TPk was not cytotoxic against HeLa and NIH-3T3 cell lines even at 100 μM (Figure 2).

CD Spectroscopy. We next determined the secondary structures of the peptides in phosphate buffer, 30 mM SDS micelles, and 1 mM EYPC/EYPG (7:3, w/w) liposomes by CD spectroscopy (Figure 3). Interpretation of CD spectra of tritrpticin and its analogues is complicated by the presence of multiple Trp aromatic side chains, preventing a detailed analysis of secondary structure (*26*). In phosphate buffer and SDS micelles, TP and its peptoid-containing peptides (TPl, TPf, and TPk) had a negative band around 225 nm, which could be caused by either the tryptophan side chains or turn structures (*8*, *9*, *27*, *28*). Interestingly, TPK exhibited two negative minimal bands at 208 and 222 nm and a positive maximal band at 195 nm in SDS micelles and EYPC/EYPG (7:3, w/w) liposomes, indicating a typical α-helical structure (*7*). Unlike SDS micelles, TPf had partially an α-helical CD pattern in the presence of EYPC/EYPG (7:3, w/w) liposomes. The α-helical structure of TPK and TPf in the membrane-mimicking environments is thought to be involved in the cytotoxicity against mammalian cells. Although TPl does not exhibit an α-helical conformation in liposomes, it is toxic to mammalian cells. We confirmed that TPf and TPl are more hydrophobic than other peptides by comparing their retention time in RP-HPLC (Table 1). It has been known that the cytotoxicity against mammalian cells of antimicrobial peptides is related to the hydrophobicity as well as α-helicity of the peptides (*29*−*33*). Therefore, the cytotoxicity of TPf and TPl can be explained by their increased hydrophobicity as well as α-helicity.

Tryptophan Fluorescence Blue Shift. To determine the local environments of the peptides, we monitored the fluorescence emission of each peptide's tryptophan residue in Tris buffer or in the presence of vesicles composed of either zwitterionic phospholipids [EYPC/cholesterol (10:1, w/w) SUVs], which mimic mammalian membranes, or negatively charged phospholipids [EYPC/EYPG (7:3, w/w) SUVs], which mimic bacterial membranes (Table 4). In the negatively charged vesicles, all of the peptides exhibited similar large blue shifts in their emission maxima, suggesting that the Trp residue in all of the peptides inserts into the more hydrophobic environment of the membrane interior. In the zwitterionic phospholipid vesicles, TP, TPl, TPf, and TPK exhibited much larger blue shifts in their emission maxima than TPk, suggesting that the Trp residue of TPk more shallowly inserts itself into the membrane interior than TP, TPl, TPf, and TPK.

Tryptophan Fluorescence Quenching Studies. To investigate the relative extent of peptide burial in the model membranes, we performed a fluorescence quenching experiment in SUVs using the water-soluble neutral fluorescence quencher acrylamide. The Stern−Volmer plots for the quenching of tryptophan recorded by acrylamide in the absence and presence of lipid vesicles are shown in Figure 4. The fluorescence of typtophan of the peptides decreased in a concentration-dependent manner via the addition of acrylamide to the peptide solution both in the absence and in the presence of liposomes. However, compared with the measurements in the absence of liposomes, the slopes were decreased in the presence of EYPC/EYPG (7:3, w/w) SUVs or EYPC/cholesterol (10:1, w/w) SUVs, suggesting that tryptophan of the peptides was buried in the bilayers, becoming inaccessible for quenching by acrylamide. In the presence of EYPC/EYPG (7:3, w/w) SUVs, all of the peptides exhibited similar extents of quenching, suggesting that their Trp residues are buried effectively in the negatively charged phospholipid membranes. In contrast, the order for the relative extent of quenching of the tryptophan fluorescence in the presence of EYPC/cholesterol (10:1, w/w) SUVs was as follows: TPk > TPK > TP ≫ TPl > TPf (suggesting the the Trp residue of TPk is less able to insert into the hydrophobic core of zwitterionic phospholipid membranes than that of TPf). In particular, the slope for TPk in the presence of EYPC/cholesterol (10:1, w/w) SUVs was much higher than in the presence of EYPC/EYPG (7:3, w/w) SUVs, suggesting TPk has a preferential interaction with negatively charged phospholipids.

Membrane Potential Depolarization. To determine the extent to which permeabilization of the cytoplasmic membrane contributed to the antibacterial activity of the peptides, we evaluated their ability to cause membrane depolarization of *S. aureus* and *E. coli* spheroplasts using the membrane potential-sensitive dye $diSC_3$-5 (Figure 5). Upon addition of the dye to a suspension of *S. aureus* and *E. coli* spheroplasts, its fluorescence was strongly quenched as it entered the membrane until levels within the membrane stabilized. Subsequent addition of peptides resulted in an increase in $diSC_3$-5 fluorescence reflecting the membrane depolarization, after which addition of gramicidin D (for *S. aureus*) or melittin (for *E. coli* spheroplasts) fully collapsed the membrane potential. TP, TPl, TPf, and TPK depolarized *S. aureus* and *E. coli* spheroplasts at a concentration of 2−4 μM,

Table 3: Cytotoxicities of the Peptides against Mammalian Cells[a]

peptide	IC_{50} (μM) HeLa	NIH-3T3
TP	70	>100
TPl	18	52
TPf	8	48
TPk	>100	>100
TPK	24	32

[a] The IC_{50} values of the peptides were determined by the MTT method (*16*).

strongly suggesting that the bacterial cytoplasmic membrane is a major target of these peptides. In contrast, TPk caused very little depolarization at a concentration of 2−4 μM (2-fold MIC), suggesting that the antibacterial activity of TPk is not due to permeabilization of the bacterial cell membrane.

Peptide-Induced Leakage of Dye from Negatively Charged LUVs. We next assessed the ability of the peptides to release the fluorescent marker calcein from bacterial cell membrane-mimicking negatively charged EYPC/EYPG (7:3, w/w) LUVs. The dose-dependent and time-dependent response curves of peptide-induced leakage of calcein from negatively charged vesicles are shown in panels A and B of Figure 6, respectively. Consistent with their respective abilities to depolarize bacterial cell membrane, TPk induced little or no calcein release at 2 μM, whereas TP, TPf, TPl, and TPK exhibited relatively strong membrane-lytic activity. Even at a high concentration of 10 μM, TPk did not cause any dye leakage. These results further confirm that, whereas membrane disruption represents a major killing event for TP, TPl, TPf, and TPK, TPk apparently exerts its bactericidal effect in some other way.

Confocal Laser-Scanning Microscopy. To determine the site of action of the peptides, we incubated Gram-negative *E. coli* and Gram-positive *S. aureus* with FITC-labeled peptides and then visualized their localization by confocal laser-scanning microscopy (Figures 7 and 8). FITC-labeled TPk penetrated the membranes and accumulated in the cytoplasm of both Gram-negative *E. coli* and Gram-positive *S. aureus*. This finding indicates that the cytoplasm and not the membrane is the major site of action of TPk. In contrast, under the same conditions, FITC-labeled TP, TPf, and TPK did not penetrate but remained associated with the membranes.

DNA Binding Activity. We next examined the DNA binding properties of the peptides to attempt to determine their molecular mechanisms of action. We determined the DNA binding affinities of the peptides by analyzing the electrophoretic mobility of DNA bands at various peptide: DNA weight ratios. TPk and TPK similarly inhibited the migration of DNA at concentrations at 2−4 μM. In contrast, TP, TPl, and TPf inhibited the migration of DNA at 8−16 μM (Figure 9).

DISCUSSION

Proline is an amino acid that creates a bend in the peptide backbone because of its cyclic structure. Thus, the Pro residue is generally thought to be an α-helix breaker. Indeed, some of the naturally occurring α-helical antimicrobial peptides, such as cecropin A, pardaxin, and PMAP-23, contain one or two Pro residues (*5*, *34*). Due to the presence of a Pro residue near the central position, such antimicrobial peptides form a unique helix−bend−helix structure (*34*−*38*). Many studies have demonstrated that a Pro residue near the central position of these α-helical antimicrobial peptides plays an important role in their bacterial cell selectivity (*36*−*44*). In a recent study, we designed antimicrobial peptides containing peptoid residues with cell selectivity by incorporating one or two Nala residues into the hydrophobic helix of a non-cell-selective ideal amphiphatic LK-rich α-helical model peptide (*45*).

Due to the presence of the two Pro residues at positions 5 and 9, tritrpticin forms a unique turn−turn structure in the membrane-mimicking SDS micelles (*9*). The first turn consists of residues 4−7, followed immediately by a second well-defined 3_{10}-helical turn consisting of residues 8−11. The hydrophobic residues are clustered together and are clearly separated from the basic Arg residues, resulting in an amphipathic structure. Peptoid residues, like proline, lack an amide nitrogen as a proton-donating group for hydrogen bonding to the peptide backbone. Thus, replacement of Pro residues with peptoid residues may also simultaneously induce a turn or a rigid bend in the secondary structure of the peptide (*46*).

In the study presented here, we synthesized tritrpticin-amide (TP) and a series of peptoid residue-substituted peptides (TPl, TPf, and TPk) to investigate the effect of Pro → peptoid residue substitution on the structure, cell selectivity, and mechanism of antibacterial action of a β-turn antimicrobial peptide such as tritrpticin (Table 1). These studies were also carried out to provide information for the

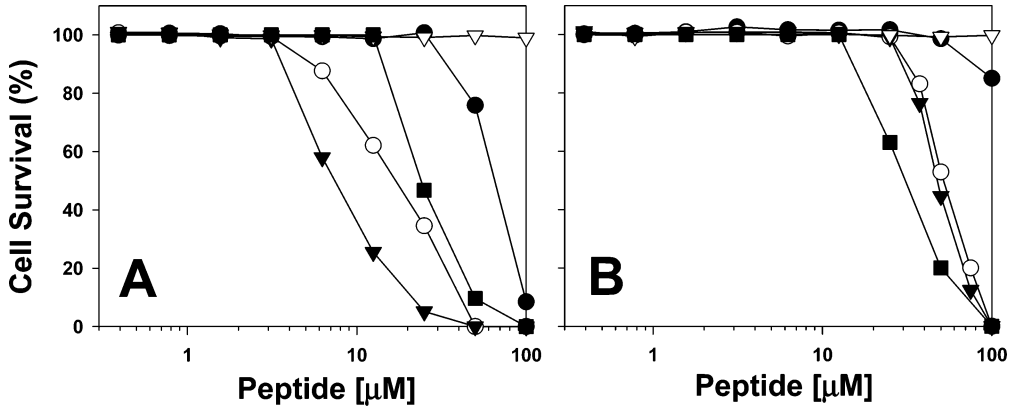

FIGURE 2: Growth inhibition dose−response curves for the peptides against HeLa cells (A) and NIH-3T3 cells (B): TP (●), TPl (○), TPf (▼), TPk (▽), and TPK (■).

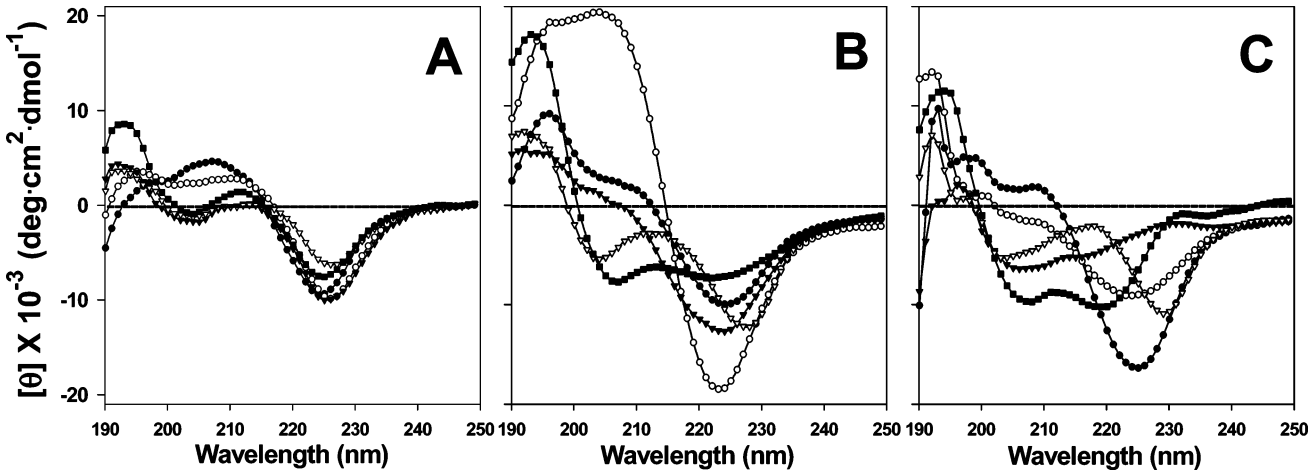

FIGURE 3: CD spectra of the peptides in 10 mM sodium phosphate buffer (pH 7.2) (A) or in the presence of 30 mM SDS (B) and 1 mM EYPC/EYPG (7:3, w/w) SUVs (C): TP (●), TPl (○), TPf (▼), TPk (▽), and TPK (■).

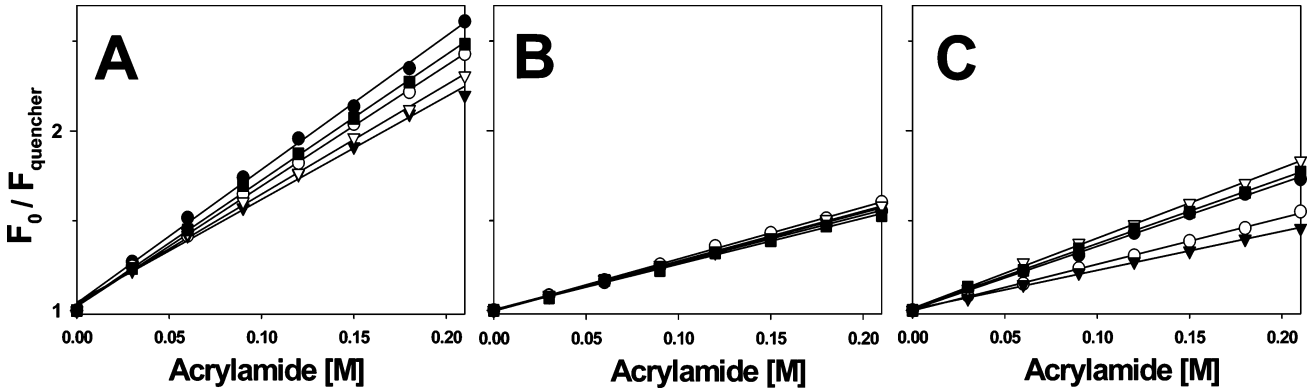

FIGURE 4: Stern−Volmer plots for the quenching of Trp fluorescence of the peptides by an aqueous quencher, acrylamide, in Tris-HCl buffer (pH 7.4) (A) or in the presence of EYPC/EYPG (7:3, w/w) SUVs (B) and EYPC/cholesterol (10:1, w/w) SUVs (C): TP (●), TPl (○), TPf (▼), TPk (▽), and TPK (■).

Table 4: Tryptophan Emission Maxima of the Peptides in Tris-HCl Buffer (pH 7.4) or in the Presence of EYPC/EYPG (7:3, w/w) Liposomes and EYPC/Cholesterol (10:1, w/w) Liposomes

peptide	Tris-HCl buffer (nm)	EYPC/EYPG (7:3, w/w) (nm)[a]	EYPC/cholesterol (10:1, w/w) (nm)[a]
TP	346.6	335.6 (11.0)	339.4 (7.2)
TPl	349.0	338.8 (10.2)	341.0 (8.0)
TPf	350.0	340.0 (10.0)	341.0 (9.0)
TPk	349.6	342.4 (7. 2)	349.4 (0.2)
TPK	349.6	339.4 (10.2)	342.6 (7.0)

[a] Blue shifts in emission maxima in parentheses.

design new short antimicrobial peptides with selectivity for bacterial cells. As for TP, we found that TPl and TPf display not only powerful antibacterial activity but also relatively strong hemolytic activity. In contrast, TPk had the most potent antimicrobial activity but lacked hemolytic activity even at 200 μM (Table 2 and Figure 1). We further examined the cytotoxicity of the peptides by testing their ability to cause the lysis of human cervical carcinoma HeLa and mouse fibroblastic NIH-3T3 cells. All of the peptides were more cytotoxic to the transformed tumor HeLa cells than the normal NIH-3T3 cells. This may be due to the presence of a higher concentration of exposed anionic phospholipids on the outer membrane surface of transformed tumor cells than on normal cells (*47*, *48*). TPl and TPf not only had the highest hemolytic activity but also were the most cytotoxic against mammalian cells, whereas TPk did not exhibit significant cytotoxicitiy against either HeLa or NIH-3T3 cells at concentrations up to at least 100 μM (Table 3 and Figure 2).

To investigate whether the selectivity of TPk toward bacterial cells is related to differences in the interaction with the outer monolayer of membranes of bacterial and mammalian cells, we performed a tryptophan fluorescence quenching study in the presence of negatively charged and zwitterionic model membranes, which mimic bacterial and mammalian membranes, respectively. Unlike TP, TPl, and TPf, TPk effectively embedded the negatively charged membrane but not the zwitterionic membrane, suggesting that the selectivity of TPk toward bacterial cells is associated with a preferential interaction with negatively charged phospholipids (Table 4 and Figure 4).

Three general mechanisms, including barrel-stave, toroidal, and carpetlike models, were originally proposed to describe the process of permeabilization of the phospholipid membranes by membrane-active peptides (*34*, *49*−*53*). In the barrel-stave model, the peptide may create transmembrane channels or pores by forming bundles of amphipathic α-helices. In this case, the hydrophobic surfaces of the peptides may interact with the hydrophobic core of the membrane, while their hydrophilic surfaces face inward, producing an aqueous pore. The toroidal model differs from the barrel-stave model in that the lipid bends back on itself like the inside of a torus. Unlike the barrel-stave model where

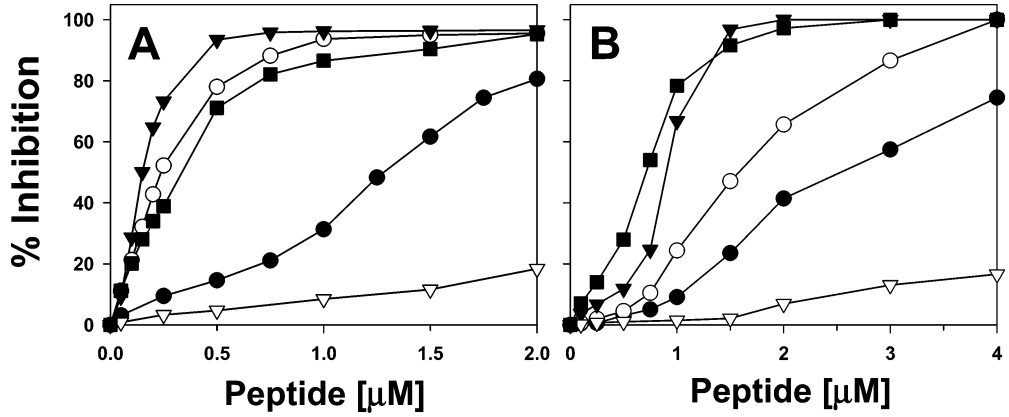

FIGURE 5: Dose−response curves of the membrane depolarization activities of the peptides against *S. aureus* (A) and *E. coli* spheroplasts (B). Membrane depolarization was monitored by an increase in the fluorescence of $diSC_3$-5 (excitation wavelength $\lambda_{ex} = 622$ nm; emission wavelength $\lambda_{em} = 670$ nm) after the addition of peptides at different concentrations: TP (●), TPl (○), TPf (▼), TPk (▽), and TPK (■).

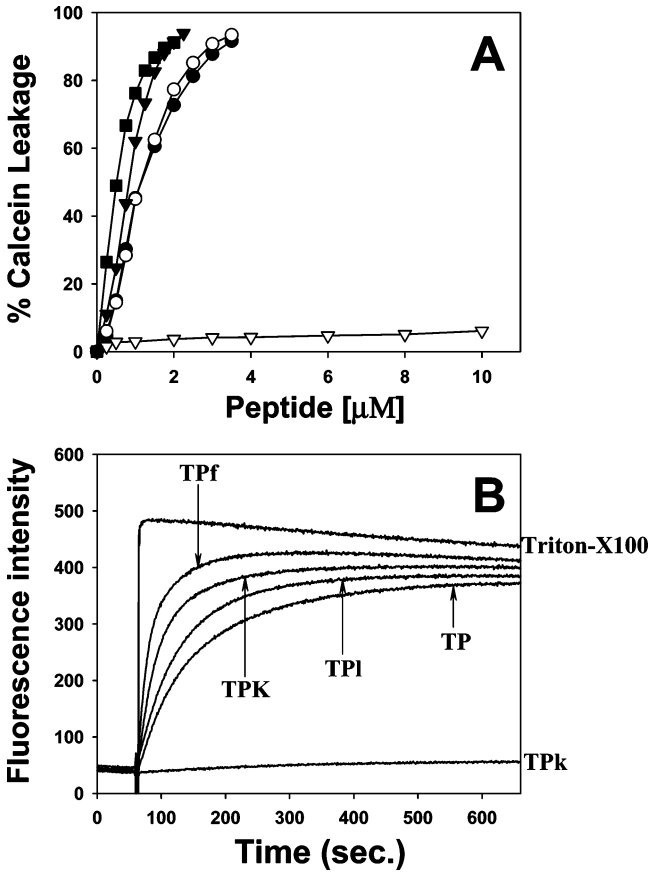

FIGURE 6: (A) Dose-dependent percent leakage of calcein from negatively charged EYPC/EYPG (7:3, w/w) LUVs at pH 7.4 measured 2 min after the addition of the peptides: TP (●), TPl (○), TPf (▼), TPk (▽), and TPK (■). (B) Time-dependent percent leakage of calcein from negatively charged EYPC/EYPG (7:3, w/w) LUVs at pH 7.4 in the presence of 2 μM peptides. The concentration of EYPC/EYPG (7:3, w/w) LUVs was 65 μM.

the peptide needs to be long enough to span the membrane, the toroidal model can be induced by smaller peptides because here the peptides probably play the role of stabilizing the lipid pore rather than lining the pore. In the carpetlike model, the peptides lie at the interface parallel to the membrane, allowing their hydrophobic surfaces to interact with the hydrophobic component of the lipid, while their positively charged residues interact with the negatively charged head groups of the phospholipid.

In contrast to membrane-active peptides, other classes of antimicrobial peptides have been suggested to target non-membrane intracellular components, such as DNA or RNA. PR-39, from porcine leucocytes (*54*), and buforin 2, from the stomach tissue of the Asian toad *Bufo bufo gargarizans* (*55*), are two peptides that penetrate cells without inducing severe membrane permeabilization. Once in the cytoplasm, they bind to and inhibit the activity of specific molecular targets essential to bacterial growth, thereby causing cell death (*55*−*60*).

To examine whether the cytoplasmic membrane of bacterial cells is the target of TPk, the abilities of the peptides to depolarize the cytoplasmic membrane of Gram-positive *S. aureus* and Gram-negative *E. coli* spheroplasts were examined by using the membrane potential-sensitive fluorescent dye $diSC_3$-5. The $diSC_3$-5 inserts into the cytoplasmic membrane under the influence of the membrane potential gradient and quenches its own fluorescence. After the addition of a peptide that forms a pore or channel or disrupts the membrane potential, the membrane potential is dissipated and the dye is released into the medium, leading to an increase in fluorescence. On the basis of the studies with this dye, TPk induced very little dissipation of the membrane potential even at levels 2-fold greater than the MIC against *S. aureus* and *E. coli* spheroplasts. In contrast, TP, TPl, TPf, and TPK caused a significant depolarization of the membrane under their MIC (Figure 5). The ability of TPk to cause leakage of a fluorescent dye entrapped within LUVs composed of negatively charged phospholipids was tested. Despite effectively binding and inserting into negatively charged phospholipids, as demonstrated by tryptophan fluorescence blue shift and quenching experiments (Table 4 and Figure 4), TPk induced very little leakage of the dye from negatively charged phospholipid vesicles even at the highest concentration that was tested (10 μM) (Figure 6). These results suggested that the bactericidal action of TPk is not due to the formation of transmembrane channels or pores or the perturbation of the cell membrane.

The inability to cause leakage of calcein from bacterial membrane-mimicking liposomes and to depolarize *S. aureus* and *E. coli* spheroplast membranes prompted us to examine whether TPk is able to penetrate bacterial cell membranes. Therefore, we used confocal laser-scanning microscopy in conjunction with FITC-labeled peptides to determine whether

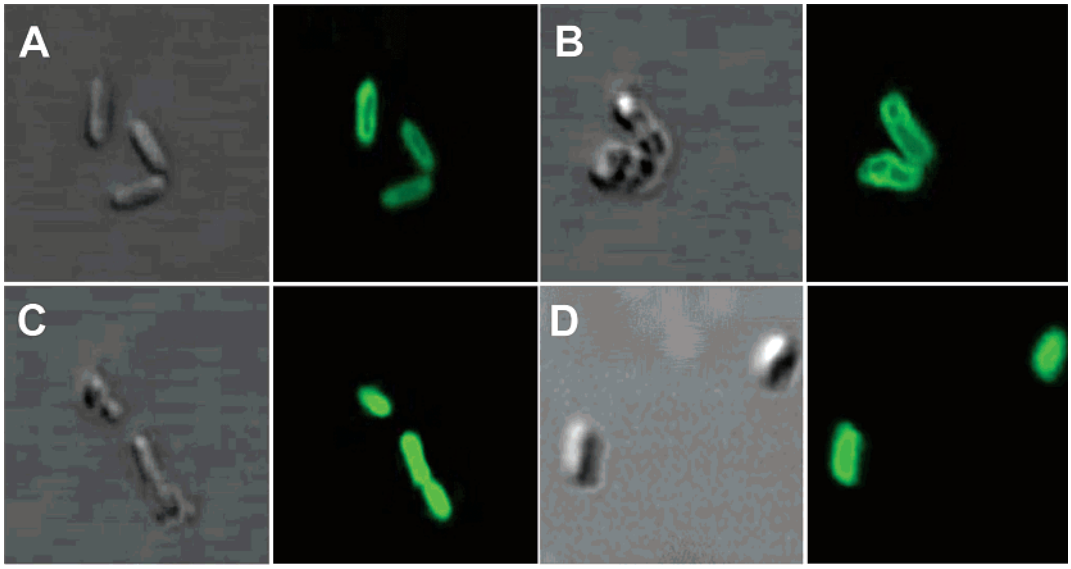

FIGURE 7: Confocal laser-scanning microscopy images of Gram-negative *E. coli* treated with FITC-labeled peptides. The cells were reacted with 5 μg/mL FITC-labeled TP (A), FITC-labeled TPf (B), FITC-labeled TPk (C), or FITC-labeled TPK (D).

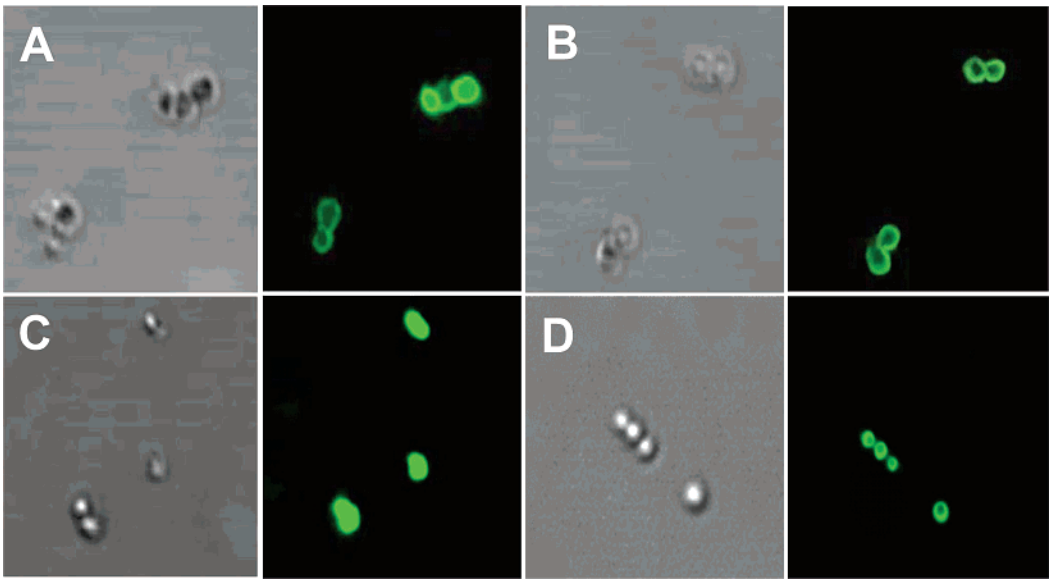

FIGURE 8: Confocal laser-scanning microscopy images of Gram-positive *S. aureus* treated with FITC-labeled peptides. The cells were reacted with 5 μg/mL FITC-labeled TP (A), FITC-labeled TPf (B), FITC-labeled TPk (C), or FITC-labeled TPK (D).

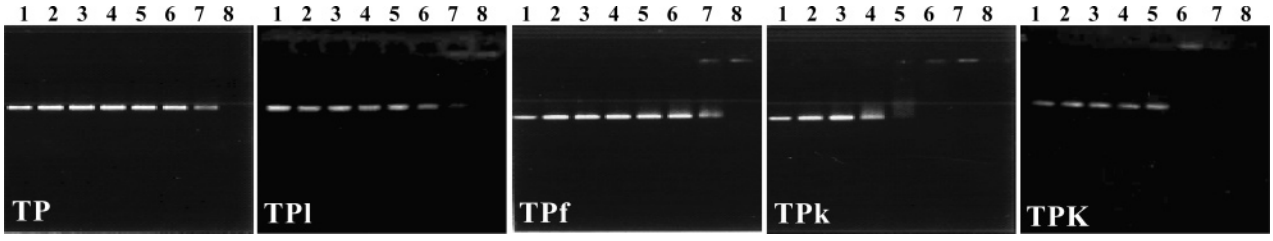

FIGURE 9: Interaction of the peptides with plasmid DNA. Binding was assayed by measuring the degree of inhibition of migration by plasmid DNA (100 ng; pBluscriptII SK^+): lane 1, plasmid DNA alone; lane 2, 0.25 μM peptide; lane 3, 0.5 μM peptide; lane 4, 1.0 μM peptide; lane 5, 2.0 μM peptide; lane 6, 4.0 μM peptide; lane 7, 8.0 μM peptide; and lane 8, 16.0 μM peptide. DNA and the peptides were co-incubated for 1 h at room temperature before electrophoresis on a 1.0% agarose gel.

the peptides penetrate bacterial cell membranes. FITC-labeled TPk penetrated the cell membrane and accumulated in the cytoplasm of both Gram-negative *E. coli* and Gram-positive *S. aureus*, whereas neither FITC-labeled TP nor FITC-labeled TPf penetrated the cell membranes. Furthermore, in the gel retardation experiment, we confirmed that TPk has a higher binding affinity for DNA. Taken together, these results indicated that TPk inhibits bacterial growth by intracellular targets like buforin 2 (*45*, *58*−*60*). Next, to investigate whether the ability of TPk to translocate across the bacterial cell membranes is due to only the increase in two positive charges, TPK with Lys at positions 5 and 9 of TP was synthesized and its biological functions were investigated. TPK induced rapid and effective leakage of dye from

bacterial membrane-mimicking liposomes, and it effectively depolarized the cytoplasmic membrane of *S. aureus* and *E. coli* spheroplasts (Figures 5 and 6). Confocal laser-scanning microscopy revealed that TPK did not penetrate the cell membrane but remained outside or on the cell membrane. As mentioned earlier, despite the peptide's backbone change by Phe peptoid residue (Nphe) substitution, TPf did not translocate across the bacterial cell membranes. Taken together, these results suggested that the ability of TPk to penetrate into the bacterial cell membranes appears to be related to the dual effects that are related to the increase in the positive charge and the peptide's backbone change by peptoid residue substitution.

In conclusion, we found that Pro → Nlys substitution (TPk) in TP significantly increased the antibacterial activity and decreased the cytotoxicity against mammalian cells, resulting in its cell selectivity. Unlike TP, TPl, TPf, and TPK, TPk caused very little dye leakage in negatively charged model membranes mimicking bacterial membranes. TPk also induced very little depolarization of the membrane potential in *S. aureus* and *E. coli* spheroplasts. Furthermore, TPk effectively penetrated the membranes of both Gram-negative *E. coli* and Gram-positive *S. aureus* and bound strongly to DNA. These results suggest that the bactericidal effect of TPk is mediated by intracellular sites rather than by disruption of the exterior membrane. Further studies to identify an intracellular site to which TPk binds may reveal the mechanism of its bactericidal action.

Collectively, our results demonstrate that a novel short antimicrobial peptide with high selectivity for bacterial cells and an intracellular mechanism of action can be generated by Pro → Nlys substitution in a Pro-containing β-turn antimicrobial peptide, such as tritrpticin. These findings help clarify the behavior of peptoid-containing antimicrobial peptides, and they provide a framework for the design of short synthetic antimicrobial peptides with optimized activity and selectivity profiles for possible therapeutic application. Finally, our findings indicate that TPk may be a suitable lead compound for the development of cell-selective antimicrobial peptides.

REFERENCES

1. Boman, H. G. (1995) Peptide antibiotics and their role in innate immunity, *Annu. Rev. Immunol. 13*, 61−92.
2. Zasloff, M. (2002) Antimicrobial peptides of multicellular organisms, *Nature 415*, 389−395.
3. Hancock, R. E., and Scott, M. G. (2000) The role of antimicrobial peptides in animal defenses, *Proc. Natl. Acad. Sci. U.S.A. 97*, 8856−8861.
4. Hancock, R. E., and Diamond, G. (2000) The role of cationic antimicrobial peptides in innate host defences, *Trends Microbiol. 8*, 402−410.
5. Andreu, D., and Rivas, L. (1998) Animal antimicrobial peptides: An overview, *Biopolymers 47*, 415−433.
6. Lawyer, C., Pai, S., Watabe, M., Borgia, P., Mashimo, T., Eagleton, L., and Watabe, K. (1996) Antimicrobial activity of a 13 amino acid tryptophan-rich peptide derived from a putative porcine precursor protein of a novel family of antibacterial peptides, *FEBS Lett. 390*, 95−98.
7. Yang, S.-T., Shin, S. Y., Kim, Y. C., Kim, Y., Hahm, K.-S., and Kim, J. I. (2002) Conformation-dependent antibiotic activity of tritrpticin, a cathelicidin-derived antimicrobial peptide, *Biochem. Biophys. Res. Commun. 296*, 1044−1050.
8. Yang, S.-T., Shin, S. Y., Lee, C. W., Kim, Y. C., Hahm, K.-S., and Kim, J. I. (2003) Selective cytotoxicity following Arg-to-Lys substitution in tritrpticin adopting a unique amphipathic turn structure, *FEBS Lett. 540*, 229−233.
9. Schibli, D. J., Hwang, P. M., and Vogel, H. J. (1999) Structure of the antimicrobial peptide tritrpticin bound to micelles: A distinct membrane-bound peptide fold, *Biochemistry 38*, 16749−16755.
10. Wu, C. W., Sanborn, T. J., Zuckermann, R. N., and Barron, A. E. (2001) Peptoid oligomer with α-chiral, aromatic side chains: Effects of chain length on secondary structure, *J. Am. Chem. Soc. 123*, 2958−2963.
11. Ng, S., Goodson, B., Ehrhardt, A., Moos, W. H., Siani, M., and Winter, J. (1999) Combinatorial discovery process yields antimicrobial peptoids, *Bioorg. Med. Chem. 7*, 1781−1785.
12. Wender, P. A., Mitchell, D. J., Pattabiraman, K., Pelkey, E. T., Steinman, L., and Rothbard, J. B. (2000) The design, synthesis, and evaluation of molecules that enable or enhance cellular uptake: Peptoid molecular transporters, *Proc. Natl. Acad. Sci. U.S.A. 97*, 13003−13008.
13. Goodman, M., Bhumralkar, Jefferson, E. A., Kwak, J., and Locardi, E. (1998) Collagen mimetics, *Biopolymers 47*, 127−142.
14. Tang, Y. C., and Deber, C. M. (2002) Hydrophobicity and helicity of membrane-interactive peptides containing peptoid residues, *Biopolymers 65*, 254−262.
15. Tang, Y. C., and Deber, C. M. (2004) Aqueous solubility and membrane interactions of hydrophobic peptides with peptoid tags, *Biopolymers 76*, 110−118.
16. Scudiero, D. A., Shoemaker, R. H., Paull, K. D., Monks, A., Tierney, S., Nofziger, T. H., Currens, M. J., Seniff, D., and Boyd, M. R. (1988) Evaluation of a soluble tetrazolium/formazan assay for cell growth and drug sensitivity in culture using human and other tumor cell lines, *Cancer Res. 48*, 4827−4833.
17. Mao, D., and Wallace, B. A. (1984) Differential light scattering and absorption flattening optical effects are minimal in the circular dichroism spectra of small unilamellar vesicles, *Biochemistry 23*, 2667−2673.
18. Shai, Y., Bach, D., and Yanovsky, A. (1990) Channel formation properties of synthetic pardaxin and analogues, *J. Biol. Chem. 265*, 20202−20209.
19. De Kroon, A. I., Soekarjo, M. W., De Gier, J., and De Kruijff, B. (1990) The role of charge and hydrophobicity in peptide-lipid interaction: A comparative study based on tryptophan fluorescence measurements combined with the use of aqueous and hydrophobic quenchers, *Biochemistry 29*, 8229−8240.
20. Zhao, H., and Kinnunen, P. K. (2002) Binding of the antimicrobial peptide temporin L to liposomes assessed by Trp fluorescence, *J. Biol. Chem. 277*, 25170−25177.
21. Papo, N., Oren, Z., Pag, U., Sahl, H.-G., and Shai, Y. (2002) The consequence of sequence alternation of amphipathic α-helical antimicrobial peptide and its diasteromers, *J. Biol. Chem. 277*, 33913−33921.
22. Sal-Man, N., Oren, Z., and Shai, Y. (2002) Preassembly of membrane-active peptides is an important factor in their selectivity toward target cells, *Biochemistry 41*, 11921−11930.
23. Shin, S. Y., Kang, S. W., Lee, D. G., Eom, S. H., Song, W. K., and Kim, J. I. (2000) CRAMP analogues having potent antibiotic activity against bacterial, fungal, and tumor cells without hemolytic activity, *Biochem. Biophys. Res. Commun. 275*, 904−909.
24. Shin, S. Y., Kang, J. H., Jang, S. Y., Kim, Y., Kim, K. L., and Hahm, K.-S. (2000) Effects of the hinge region of cecropin A(1-8)-magainin 2(1-12), a synthetic antimicrobial peptide, on liposomes, bacterial and tumor cells, *Biochim. Biophys. Acta 1463*, 209−218.
25. Shin, S. Y., Lee, S. H., Yang, S.-T., Park, E. J., Lee, D. G., Lee, M. K., Eom, S. H., Song, W. K., Kim, Y., Hahm, K.-S., and Kim, J. I. (2001) Antibacterial, antitumor and hemolytic activities of α-helical antibiotic peptide, P18 and its analogs, *J. Pept. Res. 58*, 504−514.
26. Woody, R. W. (1994) Contributions of tryptophan side chains to the far-ultraviolet circular dichroism of proteins, *Eur. Biophys. J. 23*, 253−262.
27. Nagpal, S., Gupta, V., Kaur, K. J., and Salunke, D. M. (1999) Structure-function analysis of tritrypticin, an antibacterial peptide of innate immune origin, *J. Biol. Chem. 24*, 23296−23304.
28. Yang, S.-T., Shin, S. Y., Hahm, K.-S., and Kim, J. I. (2006) Design of perfectly symmetric Trp-rich peptides with potent and broad-spectrum antimicrobial activities, *Int. J. Antimicrob. Agents 27*, 325−330.
29. Wieprecht, T., Dathe, M., Beyermann, M., Krause, E., Maloy, W. L., MacDonald, D. L., and Bienert, M. (1997) Peptide hydrophobicity controls the activity and selectivity of magainin 2 amide in interaction with membranes, *Biochemistry 36*, 6124−6132.

30. Giangaspero, A., Sandri, L., and Tossi, A. (2001) Amphipathic α-helical antimicrobial peptides, *Eur. J. Biochem. 268*, 5589−5600.
31. Yan, H., Li, S., Sun, X., Mi, H., and He, B. (2003) Individual substitution analogs of Mel(12-26), melittin's C-terminal 15-residue peptide: Their antimicrobial and hemolytic actions, *FEBS Lett. 554*, 100−104.
32. Chen, Y., Mant, C. T., Farmer, S. W., Hancock, R. E., Vasil, M. L., and Hodges, R. S. (2005) Rational design of α-helical antimicrobial peptides with enhanced activities and specificity/therapeutic index, *J. Biol. Chem. 280*, 12316−12329.
33. Zelezetsky, I., Pacor, S., Pag, U., Papo, N., Shai, Y., Sahl, H. G., and Tossi, A. (2005) Controlled alteration of the shape and conformational stability of a α-helical cell-lytic peptides: Effect on mode of action and cell specificity, *Biochem. J. 390*, 177−188.
34. Tossi, A., Sandri, L., and Giangaspero, A. (2000) Amphipathic, α-helical antimicrobial peptides, *Biopolymers 55*, 4−30.
35. Holak, T. A., Engstrom, A., Kraulis, P. J., Lindeberg, G., Bennich, H., Jones, T. A., Gronenborn, A. M., and Clore, G. M. (1988) The solution conformation of the antibacterial peptide cecropin A: A nuclear magnetic resonance and dynamical simulated annealing study, *Biochemistry 27*, 7620−7629.
36. Park, K., Oh, D., Shin, S. Y., Hahm, K.-S., and Kim, Y. (2002) Structural studies of porcine myeloid antibacterial peptide PMAP-23 and its analogues in DPC micelles by NMR spectroscopy, *Biochem. Biophys. Res. Commun. 290*, 204−212.
37. Thennarasu, S., and Nagaraj, R. (1996) Specific antimicrobial and hemolytic activities of 18-residue peptides derived from the amino terminal region of the toxin pardaxin, *Protein Eng. 9*, 1219−1224.
38. Suh, J. Y., Lee, Y. T., Park, C. B., Lee, K. H., Kim, S. C., and Choi, B. S. (1999) Structural and functional implications of a proline residue in the antimicrobial peptide gaegurin, *Eur. J. Biochem. 266*, 665−674.
39. Shin, S. Y., Park, E. J., Yang, S.-T., Jung, H. J., Eom, S. H., Song, W. K., Kim, Y., Hahm, K.-S., and Kim, J. I. (2001) Structure-activity analysis of SMAP-29, a sheep leukocytes-derived antimicrobial peptide, *Biochem. Biophys. Res. Commun. 285*, 1046−1051.
40. Oh, D., Shin, S. Y., Lee, S., Kang, J. H., Kim, S. D., Ryu, P. D., Hahm, K.-S., and Kim, Y. (2000) Role of the hinge region and the tryptophan residue in the synthetic antimicrobial peptides, cecropin A(1-8)-magainin 2(1-12) and its analogues, on their antibiotic activities and structures, *Biochemistry 39*, 11855−11864.
41. Song, Y. M., Yang, S.-T., Lim, S. S., Kim, Y., Hahm, K.-S., Kim, J. I., and Shin, S. Y. (2004) Effects of L- or D-Pro incorporation into hydrophobic or hydrophilic helix face of amphipathic α-helical model peptide on structure and cell selectivity, *Biochem. Biophys. Res. Commun. 314*, 615−621.
42. Lee, K., Shin, S. Y., Kim, K., Lim, S. S., Hahm, K.-S., and Kim, Y. (2004) Antibiotic activity and structural analysis of the scorpion-derived antimicrobial peptide IsCT and its analogs, *Biochem. Biophys. Res. Commun. 323*, 712−719.
43. Pukala, T. L., Brinkworth, C. S., Carver, J. A., and Bowie, J. H. (2004) Investigating the importance of the flexible hinge in caerin 1.1: Solution structures and activity of two synthetically modified caerin peptides, *Biochemistry 43*, 937−944.
44. Lim, S. S., Kim, Y., Park, Y., Kim, J. I., Park, I.-S., Hahm, K.-S., and Shin, S. Y. (2005) The role of the central L- or D-Pro residue on structure and mode of action of a cell-selective α-helical IsCT-derived antimicrobial peptide, *Biochem. Biophys. Res. Commun. 334*, 1329−1335.
45. Song, Y. M., Park, Y., Lim, S. S., Yang, S.-T., Woo, E.-R., Park, I.-S., Lee, J. S., Kim, J. I., Hahm, K.-S., Kim, Y., and Shin, S. Y. (2005) Cell selectivity and mechanism of action of antimicrobial model peptides containing peptoid residues, *Biochemistry 44*, 12094−12106.
46. Rainaldi, M., Moretto, V., Crisma, M., Peggion, E., Mammi, S., Toniolo, C., and Cavicchioni, G. (2002) Peptoid residues and β-turn formation, *J. Pept. Sci. 8*, 241−252.
47. Connor, J., Bucana, C., Fidler, I. J., and Schroit, A. J. (1989) Differentiation-dependent expression of phosphatidylserine in mammalian plasma membranes: Quantitative assessment of outer-leaflet lipid by prothrombinase complex formation, *Proc. Natl. Acad. Sci. U.S.A. 86*, 3184−3188.
48. Utsugi, T., Schroit, A. J., Connor, J., Bucana, C. D., and Fidler, I. J. (1991) Elevated expression of phosphatidylserine in the outer membrane leaflet of human tumor cells and recognition by activated human blood monocytes, *Cancer Res. 51*, 3062−3066.
49. Oren, Z., and Shai, Y. (1998) Mode of action of linear amphipathic α-helical antimicrobial peptides, *Biopolymers 47*, 451−463.
50. Shai, Y., and Oren, Z. (2001) From "carpet" mechanism to de-novo designed diastereomeric cell-selective antimicrobial peptides, *Peptides 22*, 1629−1641.
51. Shai, Y. (2002) Mode of action of membrane active antimicrobial peptides, *Biopolymers 66*, 236−248.
52. Papo, N., and Shai, Y. (2003) Can we predict biological activity of antimicrobial peptides from their interactions with model phospholipid membranes? *Peptides 24*, 1693−1703.
53. Ludtke, S. J., He, K., Heller, W. T., Harroun, T. A., Yang, L., and Huang, H. W. (1996) Membrane pores induced by magainin, *Biochemistry 35*, 13723−13728.
54. Agerberth, B., Lee, J. Y., Bergman, T., Carlquist, M., Boman, H. G., Mutt, V., and Jornvall, H. (1991) Amino acid sequence of PR-39. Isolation from pig intestine of a new member of the family of proline-arginine-rich antibacterial peptides, *Eur. J. Biochem. 202*, 849−854.
55. Park, C. B., Kim, M. S., and Kim, S. C. (1996) A novel antimicrobial peptide from *Bufo bufo gargarizans*, *Biochem. Biophys. Res. Commun. 218*, 408−413.
56. Boman, H. G., Agerberth, B., and Boman, A. (1993) Mechanisms of action on *Escherichia coli* of cecropin P1 and PR-39, two antibacterial peptides from pig intestine, *Infect. Immun. 61*, 2978−2984.
57. Gennaro, R., Zanetti, M., Benincasa, M., Podda, E., and Miani, M. (2002) Pro-rich antimicrobial peptides from animals: Structure, biological functions and mechanism of action, *Curr. Pharm. Des. 8*, 763−778.
58. Park, C. B., Kim, H. S., and Kim, S. C. (1998) Mechanism of action of the antimicrobial peptide buforin II: Buforin II kills microorganisms by penetrating the cell membrane and inhibiting cellular functions, *Biochem. Biophys. Res. Commun. 244*, 253−257.
59. Park, C. B., Yi, K. S., Matsuzaki, K., Kim, M. S., and Kim, S. C. (2000) Structure-activity analysis of buforin II, a histone H2A-derived antimicrobial peptide: The proline hinge is responsible for the cell-penetrating ability of buforin II, *Proc. Natl. Acad. Sci. U.S.A. 97*, 8245−8250.
60. Kobayashi, S., Takeshima, K., Park, C. B., Kim, S. C., and Matsuzaki, K. (2000) Interactions of the novel antimicrobial peptide buforin 2 with lipid bilayers: Proline as a translocation promoting factor, *Biochemistry 39*, 8648−8654.

BI060487+